THE JOURNAL OF PHYSICAL CHEMISTRY B

Article

pubs.acs.org/JPCB

Electronic Absorption Line Shapes at the Water Liquid/Vapor Interface

Katherine V. Nelson and Ilan Benjamin*

Department of Chemistry and Biochemistry, University of California, Santa Cruz, California 95064, United States

ABSTRACT: In order to investigate the factors that contribute to the electronic absorption line shape of a chromophore adsorbed at the water liquid/vapor interface, molecular dynamics simulations of a series of dipolar solutes undergoing various electronic transitions at various locations along the interface normal are studied. For electronic transitions that involve a change in the permanent dipole moment of the solute, the transition from the bulk water to the liquid/vapor interface involves a spectral shift consistent with the lower polarity of the interface. The change in the spectral width relative to that in the bulk is determined by several factors, which, depending on the nature of the transition and the dipole moment of the initial state, can result in a narrowing or broadening of the spectrum. These factors include the location of the interface region (which directly correlates with local polarity), the heterogeneity of the local solvation shell, and the width of the surface region. The contribution of the heterogeneity of the local solvation shell can be determined by comparing surface water with bulk methanol, whose polarity is comparable to one of the surface regions.

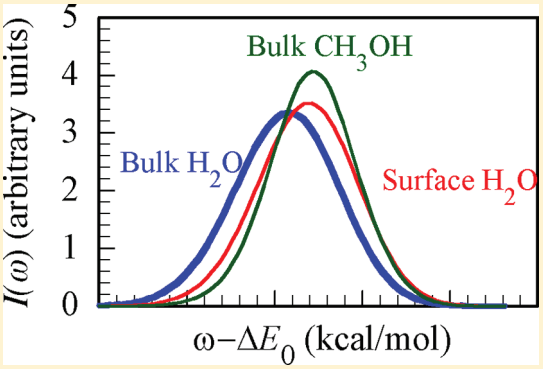

1. INTRODUCTION

In recent years, significant advances in nonlinear spectroscopic techniques, especially electronically resonant second harmonic generation (SHG) and sum frequency generation (SFG) techniques, have enabled the accurate measurement of the electronic spectra of chromophore molecules adsorbed at liquid interfaces.[1−14] These experiments, coupled with theoretical developments,[13,15−17] provide valuable information about interface structure and solvent−solute interactions. In particular, the peak spectral shift relative to the spectra in the gas phase has led to the concept of surface polarity,[5,6,9,13] which attempts to characterize the strength of solute−solvent interactions at the interface in a similar fashion to the successful polarity scale of bulk solvents.[18−22] This polarity scale is based on the observation, supported by theory, that an increase in solvent polarity results in a larger spectral shift. Several studies have explored the limitation of this concept, and in particular the dependence of the "surface polarity" on the location of the solute[9,11,12] and even its identity.[4,10,14]

Much less attention has been given to experimental studies of the spectral *width* of adsorbed solutes, which, as numerous studies in the bulk have shown,[23−30] could provide information about the orientational and translational distribution and fluctuation of the solvent molecules around the solute. This situation is in part due to the difficulty of obtaining good signal-to-noise spectra from truly interfacial molecules. While in recent years the use of broad-band nonlinear optical spectroscopic techniques has resulted in much better spectra, these cannot be directly compared with bulk absorption spectra due to their quadratic power dependence and to nonresonant background contributions to the total signal.[1,3,8,9,11,12,31]

Linearized solvation models suggest that the absorption spectral width δ of a dipolar solute in a polar solvent is related to the spectral shift $|\Delta\omega|$ (relative to the peak spectrum in vacuum) by a simple relation, $\delta^2 = CkT\Delta\omega$ (in units of $\hbar = 1$), where the constant C depends on the solute's ground and excited state dipoles but not the solvent.[24] (For example: $C = (\mu_g - \mu_e)/2\mu_g$ for the case of a solute modeled as a point dipole undergoing a parallel transition[27]). Since the spectral shift increases with solvent polarity, the width is also expected to increase with solvent polarity. Thus, when one utilizes the spectral line width to compare the degree of solvent orientational and translational distribution and fluctuation in two *different* media, one should account for the effect of solvent polarity on the width. Specifically, since the polarity of the water surface is smaller than that of bulk water, $|\Delta\omega_{surface}| < |\Delta\omega_{bulk}|$, and one would expect *spectral narrowing* if bulk and surface water have a similar range of solvent−solute configurations. Some experimental data suggest that this is indeed the case.[3,31]

Recently, Mondal et al.,[32] using heterodyne-detected electronic sum frequency generation (HD-ESFG) spectroscopy, measured the imaginary part of the second-order nonlinear susceptibility ($\mathrm{Im}[\chi^{(2)}]$) of several coumarin dyes at the water−air interface. By comparing the bandwidth of these spectra with the $\mathrm{Im}[\chi^{(1)}]$ determined from the UV spectra of the same chromophore in bulk solvents of similar polarity, (thus avoiding the need to account for the effect of polarity on the width),

Received: January 31, 2012
Revised: March 9, 2012
Published: March 12, 2012

   dx.doi.org/10.1021/jp3010037 | J. Phys. Chem. B 2012, 116, 4286−4291

they found that the spectra at the air/water interface were *broader* than those in bulk solvent and even broader than the spectrum in bulk water. This was attributed to the solute molecule sampling a wider distribution of solvent configurations at the interface than in the bulk.

Using the spectral line width to determine which medium, bulk or surface, is a more heterogeneous environment is complicated by the fact that the SFG signal is generated by all the molecules in a noncentro-symmetric medium. Since it is known from simulations, continuum models, and experiments[7,9,11−13] that the peak electronic spectrum of a chromophore depends on the chromophore's location (and orientation) along the interface normal, it is likely that molecules with different spectral shifts contribute to the observed signal. Therefore, it is not clear to what degree the observed width is due to intrinsic local heterogeneity or due to the fact that the observed spectrum is a sum of shifted spectra. In this paper we consider this question in detail with the help of a simple model of a dipolar solute adsorbed at different locations of the water liquid/vapor interface.

Previous calculations of spectral line width of adsorbed solutes at interfaces were limited to a few simulations[15,16] and a continuum model,[17] but no systematic investigation of this issue was attempted. For a very recent discussion of interfacial line width in a simple nonpolar solvent, that addresses the problem of the contribution of molecules across the interfacial region, see ref 33.

The rest of the paper is organized as follows: In section 2, we discuss the simple dipolar model. In section 3, we give simulation details. The results are discussed in section 4, and concluding remarks are in section 5.

2. A DIPOLAR SOLUTE MODEL

The model we use to describe the electronic transition $|i\rangle \rightarrow |f\rangle$ includes a dipolar solute constrained to be at different locations of the water liquid/vapor interface or in bulk water and in bulk methanol. The solute is described by two identical atoms rigidly held at a bond distance of R_{eq} = 4 Å, using the SHAKE algorithm.[34] The two atoms carry partial charges $+Q_i$ and $-Q_i$ in the initial electronic state and $+Q_f$ and $-Q_f$, respectively, in the final state. We study 64 different dipole parallel transitions by selecting the partial charges Q_i and Q_f to be all possible combinations of the values 0, 0.1, 0.2, ..., 0.7 in atomic units. These choices give rise to dipole moment values in the range of commonly studied chromophores. The solute atoms interact with water via Lennard-Jones plus Coulomb terms. For simplicity, the Lennard-Jones parameters of the two atoms are taken to be the same and equal to σ_i = 3 Å and ε_i = 0.2 kcal/mol. In addition, we assume that these values are identical in the initial and final electronic states for all the transitions considered. However, some calculations were done where the polarizability of the final state was larger by selecting $\varepsilon_f = 2\varepsilon_i$. This increase in the effective solute polarizability is consistent with typical experimental systems, such as the $\pi \rightarrow \pi^*$ transition in aromatic compounds.[20]

Thus, the potential energy surfaces of the initial and final states are

$$H_i = U_w + U_i^{LJ} + U_i^{Coul}$$
$$H_f = \Delta E_0 + U_w + U_f^{LJ} + U_f^{Coul} \quad (1)$$

In eq 1, ΔE_0 is the vacuum energy difference between the final and initial states. U_w is the total water intermolecular and intramolecular potential energy surfaces, described using the flexible SPC model,[35] which has been shown to give reasonable bulk and interfacial properties.[36,37] U_ν^{LJ} and U_ν^{Coul} are the solute−water Lennard-Jones and Coulomb interaction energies, respectively, in the state ν ($\nu = i$ or f). These are explicitly given by

$$U_\nu^{LJ} = 4\sqrt{\varepsilon_\nu \varepsilon_O} \sum_{n=1}^{N} \left[\left(\frac{\sigma}{r_{1n}}\right)^{12} - \left(\frac{\sigma}{r_{1n}}\right)^{6} + \left(\frac{\sigma}{r_{2n}}\right)^{12} - \left(\frac{\sigma}{r_{2n}}\right)^{6} \right] = \sqrt{\varepsilon_\nu}\,\Omega(\mathbf{r})$$
$$U_\nu^{Coul} = Q_\nu \sum_{n=1}^{3N} q_n [r_{1n}^{-1} - r_{2n}^{-1}] = Q_\nu \Gamma(\mathbf{r}) \quad (2)$$

where r_{jn} is the distance between a solute atom j (j = 1 or 2) and a water site n (an oxygen atom in the case of the Lennard-Jones term, and an oxygen or a hydrogen atom in the case of the Coulomb term), $\sigma = (\sigma_O + \sigma_j)/2$ with the water SPC parameters σ_O = 3.165 Å and ε_O = 0.155 kcal/mol, and q_n is the charge in atomic units on the nth water site. In eq 2 we made use of the standard Lorentz−Berthelot mixing rules for the Lennard-Jones interaction parameters between two different atomic sites.[38] Note that $\Omega(\mathbf{r})$ and $\Gamma(\mathbf{r})$ depend on the instantaneous nuclear configuration, but not on the electronic state.

The above calculations are also carried out in bulk methanol in order to compare the interface spectra with the spectra in a bulk medium of a similar polarity. The model used is a three-site Lennard-Jones plus Coulomb potential, with parameters given in ref 39, so expressions similar to those given in eq 2 can be written in this case as well.

Neglecting solvent dynamics and assuming an infinite excited-state lifetime and the Franck−Condon approximation, the normalized static line shape is given by the distribution of energy gaps between the final and initial states governed by the initial state Hamiltonian:[23,25−27,29,30]

$$I_{i\rightarrow f}(\omega) = \langle \delta[\omega - \Delta E_0 - \Delta U(\mathbf{r})] \rangle_i$$
$$\Delta U(\mathbf{r}) = (\sqrt{\varepsilon_f} - \sqrt{\varepsilon_i})\Omega(\mathbf{r}) + (Q_f - Q_i)\Gamma(\mathbf{r}) \quad (3)$$

(in units of $\hbar = 1$), where δ is the Dirac delta function, and $\langle ... \rangle_i = (\int e^{-\beta H_i} ... d\mathbf{r})/(\int e^{-\beta H_i} d\mathbf{r})$ represents the canonical ensemble average in the initial state and $\beta = 1/kT$. By running molecular dynamics or Monte Carlo simulations with the Hamiltonian H_i and binning the instantaneous energy gap, one obtains the absorption or emission line shape in the static inhomogenous limit.[15,16,27,29,30,40]

Note that if the delta function in eq 1 is replaced by its Fourier representation, $\langle \delta(\omega - \Delta E) \rangle = (2\pi)^{-1} \int_{-\infty}^{\infty} e^{-i\omega t} \langle e^{i\Delta E t} \rangle dt$, and $\langle e^{i\Delta E t} \rangle$ is approximated by a

dx.doi.org/10.1021/jp3010037 | J. Phys. Chem. B 2012, 116, 4286−4291

second-order expansion,[27,29,41] one obtains a Gaussian line shape:

$$I_{i\to f}(\omega) = \frac{1}{\sqrt{2\pi\delta^2}} e^{-(\omega-\Delta E_0-\Delta\omega)^2/2\delta^2}$$
$$\Delta\omega = \langle \Delta U\rangle_i$$
$$\delta^2 = \langle (\Delta U)^2\rangle_i - \langle \Delta U\rangle_i^2 \quad (4)$$

Equation 4 can be used as the starting point of several statistical mechanics[27,29,41−43] or continuum models'[17,24,28,44−46] approximate theories of line shape, but here we use direct binning of the energy gap to compute the exact line shape (in the static Franck−Condon limit). Note also that because of the pair approximation of the total potential energy function, a simulation of one initial state can provide the line shape for transitions to multiple final states, as long as the probability distribution of the quantities U_i^{LJ} and U_i^{Coul} (or, equivalently $\Gamma(\mathbf{r})$ and $\Omega(\mathbf{r})$) are known.

3. SIMULATION DETAILS

The simulation system includes 1000 water molecules in a rectangular box of cross section 31.3 Å × 31.3 Å and a diatomic solute molecule, which is adsorbed at different locations of the water liquid/vapor interface and in bulk water. Periodic boundary conditions are used in all three dimensions, with a molecule-based continuous force-switching function at half the box length, and a reaction field correction for the long-range electrostatic forces.[47] The simulations in bulk methanol used 215 molecules in a truncated octahedron (TO) box, whose enclosing cube has a size of 30.74 Å. (The volume of the TO box is half the volume of the defining cube).

The geometry of the system leads to two liquid vapor interfaces with the Gibbs dividing surface located at ±15 Å. (This is the plane perpendicular to the Z-axis, where the excess water on the bulk side is equal to the decrease on the vapor side,[48,49] which is approximately where the water density is half the bulk value). Because of the complete symmetry with respect to the box midpoint, one may use both surfaces to study the solute spectra, but we present the results using the positive half of the system (see Figure 1 for the density profile). To obtain statistically accurate spectra for the solute located in different slabs parallel to the interface, we constrain the center of mass of the solute using a window potential given by

$$U_w(z) = k_w\theta(x)x^2, \quad x = |z - Z_{cm}| - h \quad (5)$$

where k_w is a force constant on the order of 10^3 kcal/mol/Å (the exact value is not important), and $\theta(x)$ is the unit step function ($\theta(x) = 0$ if $x < 0$; $\theta(x) = 1$ if $x > 0$). Thus the solute is free to move inside a slab of thickness h (selected to be 2 Å) centered at Z_{cm}. We select Z_{cm} = 0, 13, 15, 17, and 19 Å. These locations are labeled B, G−, G, G+, and G++, respectively (see Figure 1).

The temperature in all the calculations is 298 K. The equations of motion are integrated using the velocity Verlet algorithm[47] with a time step of 0.5 fs.

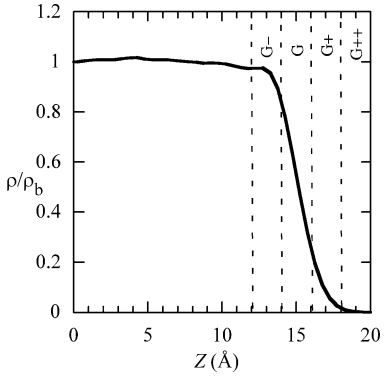

Figure 1. The density profile of an FSPC water/vapor interface at 298 K. Depicted are the different surface regions in which a chromophore is located.

4. RESULTS AND DISCUSSION

In this section we first discuss the results for one particular "electronic" transition, then show the combined data for all the transitions investigated. For an electronic transition that involves only a change in the charge distribution $Q_i \to Q_f$, the shift in the peak position of the spectrum of the solute adsorbed at the location z relative to the peak position when the solute is in the bulk is approximately given by combining eqs 3 and 4:

$$\Delta\omega(z) - \Delta\omega(0) = (Q_f - Q_i)[\langle\Gamma_z(\mathbf{r})\rangle_i - \langle\Gamma_0(\mathbf{r})\rangle_i] \quad (6)$$

(The relation is exact if the spectrum shape is symmetrical). Since the expression inside the square parentheses is typically positive (polar solute−water electrostatic interaction energies are less negative when the solute is at the interface than in the bulk), transitions that involve an increase in the solute electric dipole ($Q_f > Q_i$) are shifted to higher energies at the surface.

The top panel of Figure 2 shows, as an example, the calculated spectra for one particular "electronic" transition (Q_i = 0.2 → Q_f = 0.7) of the solute adsorbed at different water surface locations and in bulk water. As expected, there is a shift to the "blue" when the solute is moved from bulk water to the interface, which is also found experimentally. However, there is a slight *narrowing* of the spectra as the solute is moved to the lower density (and polarity) interface regions. While this is qualitatively consistent with the linear response relation between the peak width and shift mentioned earlier ($\delta \propto (|\Delta E|)^{1/2}$), it clearly suggests that any increase in inhomogeneous broadening due to a more heterogeneous environment is smaller than the narrowing expected because of the reduced polarity.

The significant dependence of the spectrum's peak location on the solute Z-location presents a difficulty when comparing calculated and experimental spectral shift and width, since in reality, the adsorbed solute will sample all locations with a probability that is reflected by its local free energy profile. The spectrum will be a weighted average of all locations that are in the non centro-symmetric region. Since the adsorption behavior of the simple dipolar solute in our model is not expected to follow that of the experimentally studied chromophore, we instead show in the bottom panel of Figure 2 two other spectra calculated by taking a wider slice of the interface than the individual slices shown in the top panel. The "narrow" interface spectrum (labeled NI) is obtained by including locations G−, G, and G+, and the "broad" interface (labeled BI) also includes the G++ location. The peak positions of these spectra are, as expected, close to the average of the

dx.doi.org/10.1021/jp3010037 | J. Phys. Chem. B 2012, 116, 4286−4291

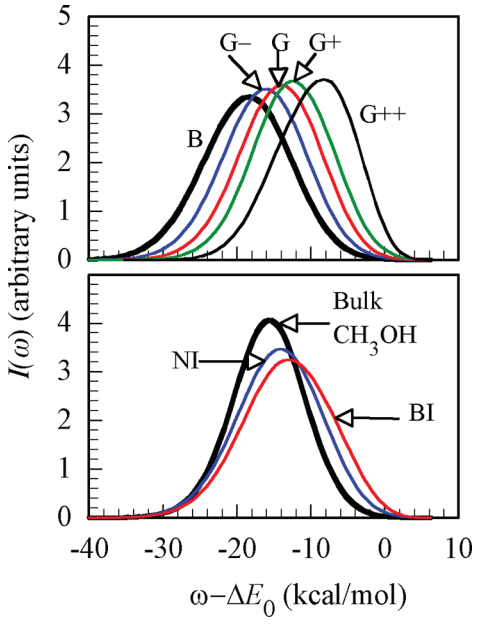

Figure 2. Top panel: Electronic absorption spectra (normalized to the same area) for the transition: $Q_i = 0.2 \rightarrow Q_f = 0.7$ of a chromophore at different locations of the water liquid/vapor interface and in bulk water. Bottom panel: The spectra for the same transition in bulk methanol and at two composite interface regions, as defined in the text.

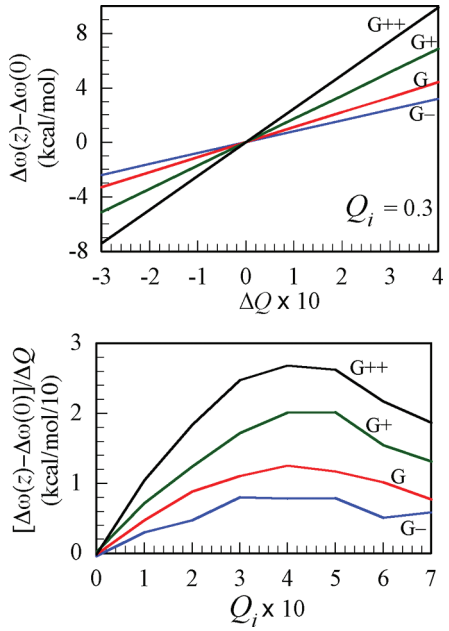

Figure 3. Top panel: The spectral shift relative to the bulk, $\Delta\omega(z) - \Delta\omega(0)$, versus the change in the solute charge ΔQ for one specific choice of the initial solute charge at the different solute surface locations. Bottom panel: The slope $[\Delta\omega(z) - \Delta\omega(0)]/\Delta Q$ versus the initial solute charge for all solute surface locations.

spectra from the individual slabs. Now, however, one does obtain a slightly *broader* surface spectrum when one combines the contributions from a wider interface region, as is shown in the bottom panel of Figure 2.

Using the spectral width to compare the heterogeneity of two different media is appropriate when their polarity is similar. This was demonstrated experimentally by measuring the absorption spectra in bulk organic solvents whose polarity is similar to that of surface water. Following this approach, the bottom panel of Figure 2 shows the spectrum calculated for the $Q_i = 0.2 \rightarrow Q_f = 0.7$ transition (same solute) in bulk methanol. For this case, the spectral shift suggests that bulk methanol's effective polarity is similar to that of region G− of the water liquid/vapor interface. The bulk methanol spectrum is narrower than the corresponding spectrum in the G− region, which is consistent with a lower degree of heterogeneity of the bulk compared with the surface and with the experimental observation.

Turning next to a discussion of all the transitions examined, we note from eq 6 that for a given initial state (characterized by a given value of Q_i), the spectral shift relative to the bulk, $\Delta\omega(z)-\Delta\omega(0)$, is linear in ΔQ. This is demonstrated in the top panel of Figure 3 for a particular choice of Q_i, for all solute surface locations. The slope $[\Delta\omega(z) - \Delta\omega(0)]/\Delta Q$ increases as the solute is moved to a lower polarity region simply because the dehydration increases relative to the bulk. Since the slope for a given surface location depends on Q_i alone, the bottom panel depicts the slope versus Q_i for all solute surface locations. Interestingly this plot exhibits a maximum for each solute location at $Q_i = 4$. This is due to the effect of two competing factors: As Q_i increases from zero, the weaker hydration relative to the bulk becomes more pronounced. However, for large enough values of Q_i, the tightening of the solute's hydration shell as it is moved to the interface ("electrostriction") reduces the difference in the total solute/water interaction energy. Obviously, each of these two effects is most pronounced in the G++ region. The diminished surface effect due to this "electrostriction" effect has consequences for many other solute properties.[50]

We next summarize the results for the spectral width of all the transitions at all locations. Assuming the spectral line shapes are Gaussians, eqs 3 and 4 show that the spectral line width for the $Q_i \rightarrow Q_f$ transition is given by:

$$\delta = (Q_f - Q_i)\sqrt{\langle\Gamma^2(\mathbf{r})\rangle_i - \langle\Gamma(\mathbf{r})\rangle_i^2} \tag{7}$$

Given δ_s and δ_b, the width of the spectrum when the solute is at some interface location and in the bulk, respectively, we are interested in the relative change in width:

$$\frac{\delta_s - \delta_b}{\delta_b} = \frac{\sqrt{\langle\Gamma_s^2(\mathbf{r})\rangle_i - \langle\Gamma_s(\mathbf{r})\rangle_i^2}}{\sqrt{\langle\Gamma_b^2(\mathbf{r})\rangle_i - \langle\Gamma_b(\mathbf{r})\rangle_i^2}} - 1 \tag{8}$$

where Γ_s and Γ_b are defined in eq 2 and calculated when the solute's center of mass is located at the surface and in the bulk, respectively. Note that the expression in eq 8 is independent of the final electronic state. A negative value of this quantity corresponds to spectral narrowing relative to the bulk. Figure 4 depicts the relative change $(\delta_s - \delta_b)/\delta_b$ versus Q_i for all locations. The top panel of Figure 4 shows that the example discussed earlier reflects the general case: there is a significant narrowing for most transitions, especially those that correspond to an initial state with a small dipole. Initial states with large dipoles do not have much change in the spectral width (for transitions to any final state). This reflects the relatively small change in the local environment of such a solute when it is moved from the bulk to the interface. We conclude that if there is any broadening due to an increase in the heterogeneity of the local solute environment, it is smaller than the narrowing expected from the reduced polarity (according to linear

dx.doi.org/10.1021/jp3010037 | J. Phys. Chem. B 2012, 116, 4286−4291

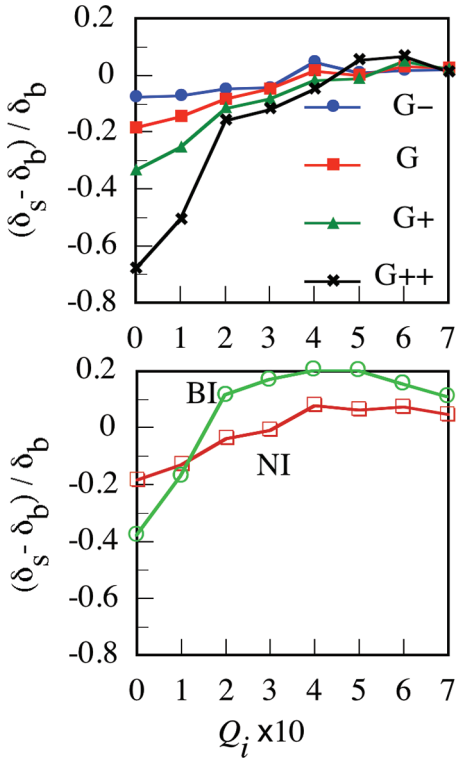

Figure 4. The change in the spectral width of the electronic transition at the interface relative to the bulk versus the initial solute charge. The top panel shows the results at different surface locations, and the bottom panel shows results at two composite interface regions, as defined in the text.

response). Experimental observations of broader surface spectra in *the same solvent* could be due to the sampling of a wider region. In this case, the superposition of spectra with significantly different peak positions could produce a broad spectrum. This is demonstrated in the bottom panel of Figure 4.

It is worth noting that the "heterogeneity in the local environment" mentioned above is expected to increase at the interface due to the rapid variation in the intermolecular interactions along the interface normal, as well as the dependence of these interactions on the solute orientation. While in the bulk the average intermolecular potential experienced by the solute is orientation-independent, this is not so at the interface. However, the dependence of the degree of heterogeneity on the solute dipole is not simple. An increase in the solute's dipole will increase the asymmetry in the effective angle-dependent potential experienced by the solute, but at the same time will likely limit the range of observed orientations around the most likely solute surface orientation.

Finally, we consider electronic transitions that involve a change in the solute polarizability. We model these transitions by increasing the value of the parameter ε in the Lennard-Jones potential energy function of the excited electronic state by a factor of 2. The energy differences corresponding to this change are significantly smaller than those that involve a change in the permanent dipole moment, so we limit our discussion (of the effect on the spectral width) to the case where there is no change in the dipole moment, $Q_i = Q_f$. From eqs 3 and 4 we note that for this case

$$\Delta\omega(z) = (\sqrt{\varepsilon_f} - \sqrt{\varepsilon_i})[\langle\Omega_z(\mathbf{r})\rangle_i] \quad (9)$$

where $\Omega_z(\mathbf{r})$ is given by the first term in eq 2, calculated when the solute center of mass is located in a slab centered at the location z along the interface normal. Note that the quantity inside the square brackets of eq 9 is proportional to the average Lennard-Jones contribution to the total solvent–solute interaction energy in the initial state: $\langle\Omega_z(\mathbf{r})\rangle_i = \langle U_i^{LJ}(\mathbf{r})\rangle_i / (\varepsilon_i)^{1/2}$. From this expression, we see that $\langle\Omega_z(\mathbf{r})\rangle$ is negative if the solute solvent configurations are mostly near the minimum of the Lennard-Jones potential. This is the case when the Coulomb interactions in the initial state are weak (a small value of Q_i). However, for a large Q_i, the strong electrostatic attractions put the most probable solvent–solute distance on the repulsive side of the Lennard-Jones potential, and $\langle\Omega_z(\mathbf{r})\rangle$ becomes positive and increases as Q_i increases.

Figure 5 summarizes the results. The top panel shows that for small values of the initial solute charge, the spectral shift

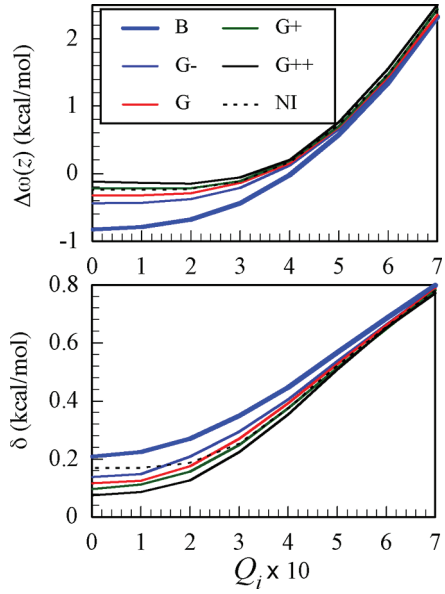

Figure 5. Top panel: The spectral shift $\Delta\omega(z)$ versus the (fixed) solute charge for all solute surface locations (as indicated) for a solute undergoing a change in the electronic polarizability. Bottom panel: The corresponding spectral width.

relative to the gas phase is negative and gets smaller in value as the solute is moved from the bulk to the interface. As the initial charge Q_i increases, the shift become positive, consistent with the above discussion regarding the sign of the quantity $\langle\Omega_z(\mathbf{r})\rangle$. As the solute is transferred from the bulk to the interface, the number of nearest neighbors is reduced due to the lower density, which makes $\langle|\Omega_z(\mathbf{r})|\rangle$ smaller. However, this effect is diminished as Q_i increases, since the solute's ability to keep the local solute hydration shell intact increases.

The bottom panel shows the width of the spectra versus Q_i in all the regions. The increase in width with increasing value of Q_i suggests an increase in the degree of fluctuations in the local hydration shell. This does not represent an increase in heterogeneity but rather the fact that fluctuations in the solute–water distance around the equilibrium value result in larger energy fluctuations when the equilibrium distance is located on the repulsive side of the Lennard-Jones potential. For a given value of Q_i, the spectral width decreases as the solute is moved from the bulk to the surface because of the decrease in the number of the water molecules in the solute

dx.doi.org/10.1021/jp3010037 | J. Phys. Chem. B 2012, 116, 4286–4291

hydration shell. Again, this effect diminishes when Q_i increases because of the tightening of the hydration shell.

We conclude that transitions involving a change in solute polarizability at a fixed permanent solute dipole give rise to a spectral narrowing when comparing bulk and surface spectra, although the effect is small and gets smaller when the size of the solute dipole increases. However, as in the case of transitions that involve a change in the solute dipole, some broadening is expected when the solute is allowed to explore a wider surface region. This gives rise to some broadening, but it is still narrower than the spectral width in the bulk.

5. CONCLUSIONS

Our model calculations suggest that three factors contribute to the difference between the bulk and interface electronic spectral line width of a chromophore undergoing a change in its permanent dipole moment: local solvation shell heterogeneity, polarity of the interface region, and the width of the surface region accessible to the solute. The local solute environment is more heterogeneous at the interface, which leads to spectral broadening. However, the reduced polarity of the interface region leads to a spectral narrowing, which typically is more pronounced. This leads to overall narrowing when the spectrum of the solute in the bulk is compared with the spectrum taken when the solute is restricted to a narrow surface slab. The spectrum obtained when several surface slabs contribute to the electronic transition is wider. The dependence of the spectral shift and width on the initial solute charge can be understood by invoking the idea that the structure of the solute hydration shell at the interface resembles that in the bulk as the solute charge is increased.

AUTHOR INFORMATION

Notes

The authors declare no competing financial interest.

ACKNOWLEDGMENTS

This work was supported by the National Science Foundation (Grant CHE-0809164).

REFERENCES

(1) Shen, Y. R. *The Principles of Nonlinear Optics*; Wiley: New York, 1984.
(2) Eisenthal, K. B. *Chem. Rev.* **1996**, *96*, 1343.
(3) Tamburello-Luca, A. A.; Hébert, P.; Brevet, P. F.; Girault, H. H. *J. Chem. Soc., Faraday Trans.* **1996**, *92*, 3079.
(4) Tamburello-Luca, A. A.; Hébert, P.; Antoine, R.; Brevet, P. F.; Girault, H. H. *Langmuir* **1997**, *13*, 4428.
(5) Wang, H.; Borguet, E.; Eisenthal, K. B. *J. Phys. Chem.* **1997**, *101*, 713.
(6) Wang, H. F.; Borguet, E.; Eisenthal, K. B. *J. Phys. Chem. B* **1998**, *102*, 4927.
(7) Steel, W. H.; Nolan, R.; Damkaci, F.; Walker, R. A. *J. Am. Chem. Soc.* **2002**, *124*, 4824.
(8) Zhang, X. Y.; Cunningham, M. M.; Walker, R. A. *J. Phys. Chem. B* **2003**, *107*, 3183.
(9) Steel, W. H.; Walker, R. A. *Nature* **2003**, *424*, 296.
(10) Steel, W. H.; Walker, R. A. *J. Am. Chem. Soc.* **2003**, *125*, 1132.
(11) Steel, W. H.; Beildeck, C. L.; Walker, R. A. *J. Phys. Chem. B* **2004**, *108*, 16107.
(12) Steel, W. H.; Lau, Y. Y.; Beildeck, C. L.; Walker, R. A. *J. Phys. Chem. B* **2004**, *108*, 13370.
(13) Benjamin, I. *Chem. Rev.* **2006**, *106*, 1212.
(14) Siler, A. R.; Walker, R. A. *J. Phys. Chem. C* **2011**, *115*, 9637.
(15) Michael, D.; Benjamin, I. *J. Chem. Phys.* **1997**, *107*, 5684.
(16) Michael, D.; Benjamin, I. *J. Phys. Chem.* **1998**, *102*, 5154.
(17) Benjamin, I. *J. Phys. Chem. A* **1998**, *102*, 9500.
(18) Kamlet, M. J.; Abboud, J. L.; Taft, R. W. In *Progress in Physical Organic Chemistry*; Cohen, S. G., Streitwieser, A., Taft, R. W., Eds.; Wiley: New York, 1981; Vol. *13*; p 485.
(19) Reichardt, C. *Solvents and Solvent Effects in Organic Chemistry*, 2nd ed.; Springer-Verlag: Weinheim, Germany, 1988.
(20) Reichardt, C. *Chem. Rev.* **1994**, *94*, 2319.
(21) Laurence, C.; Nicolet, P.; Dalati, M. T.; Abboud, J. L. M.; Notario, R. *J. Phys. Chem.* **1994**, *98*, 5807.
(22) Matyushov, D. V.; Schmid, R.; Ladanyi, B. M. *J. Phys. Chem. B* **1997**, *101*, 1035.
(23) Kubo, R. *J. Phys. Soc. Jpn.* **1962**, *17*, 1100.
(24) Marcus, R. A. *J. Chem. Phys.* **1965**, *43*, 1261.
(25) Mataga, N.; Kubota, T. *Molecular Interactions and Electronic Spectra*; Dekker: New York, 1970.
(26) Loring, R. F. *J. Phys. Chem.* **1990**, *94*, 513.
(27) Shemetulskis, N. E.; Loring, R. F. *J. Chem. Phys.* **1991**, *95*, 4756.
(28) Ågren, H.; Mikkelsen, K. V. *J. Mol. Struct. (THEOCHEM)* **1991**, *234*, 425.
(29) Sevian, H. M.; Skinner, J. L. *J. Chem. Phys.* **1992**, *97*, 8.
(30) Bader, J. S.; Berne, B. J. *J. Chem. Phys.* **1996**, *104*, 1293.
(31) Zimdars, D.; Eisenthal, K. B. *J. Phys. Chem. B* **2001**, *105*, 3993.
(32) Mondal, S. K.; Yamaguchi, S.; Tahara, T. *J. Phys. Chem. C* **2011**, *115*, 3083.
(33) Benjamin, I. *Chem. Phys. Lett.* **2011**, *515*, 56.
(34) Ryckaert, J. P.; Ciccotti, G.; Berendsen, H. J. C. *J. Comput. Phys.* **1977**, *23*, 327.
(35) Berendsen, H. J. C.; Postma, J. P. M.; Gunsteren, W. F. V.; Hermans, J. In *Intermolecular Forces*; Pullman, B., Ed.; D. Reidel: Dordrecht, The Netherlands, 1981; p 331.
(36) Benjamin, I. Molecular dynamics simulations in interfacial electrochemistry. In *Modern Aspects of Electrochemistry*; Bockris, J. O. M., Conway, B. E., White, R. E., Eds.; Plenum Press: New York, 1997; Vol. *31*; p 115.
(37) Michael, D.; Benjamin, I. *J. Chem. Phys.* **2001**, *114*, 2817.
(38) Hansen, J.-P.; McDonald, I. R. *Theory of Simple Liquids*, 2nd ed.; Academic: London, 1986.
(39) Benjamin, I. *Phys. Rev. Lett.* **1994**, *73*, 2083.
(40) Benjamin, I. *Chem. Phys. Lett.* **2004**, *393*, 453.
(41) Stephens, M. D.; Saven, J. G.; Skinner, J. L. *J. Chem. Phys.* **1997**, *106*, 2129.
(42) Chandler, D.; Schweizer, K. S.; Wolynes, P. G. *Phys. Rev. Lett.* **1982**, *49*, 1100.
(43) Chen, Y. C.; Lebowitz, J.; Nielaba, P. *J. Chem. Phys.* **1989**, *91*, 340.
(44) Mirashi, L. S. P.; Kunte, S. S. *Spectrochim. Acta* **1989**, *45A*, 1147.
(45) Kim, H. J.; Hynes, J. T. *J. Chem. Phys.* **1990**, *93*, 5194.
(46) Kim, H. J.; Hynes, J. T. *J. Chem. Phys.* **1990**, *93*, 5211.
(47) Allen, M. P.; Tildesley, D. J. *Computer Simulation of Liquids*; Clarendon: Oxford, 1987.
(48) Rowlinson, J. S.; Widom, B. *Molecular Theory of Capillarity*; Clarendon: Oxford, 1982.
(49) Nicholson, D.; Parsonage, N. G. *Computer Simulation and the Statistical Mechanics of Adsorption*; Academic Press: New York, 1982.
(50) Benjamin, I. *Chem. Phys. Lett.* **2009**, *469*, 229.